

1 Article

2

Insights into the Voltage Regulation Mechanism of

3

the Pore-Forming Toxin Lysenin

4 **Sheenah Lynn Bryant^{1,2}, Tyler Clark¹, Christopher Alex Thomas¹, Kaitlyn Summer Ware¹,**
5 **Andrew Bogard^{1,2}, Colleen Calzacorta¹, Daniel Prather¹, Daniel Fologea^{1,2,*}**6 ¹ Department of Physics, Boise State University, Boise, ID 83725, USA7 ² Biomolecular Sciences Graduate Program, Boise State University, Boise, ID 83725, USA

8 * Correspondence: DanielFologea@boisestate.edu; Tel.: +1-208-426-2664

9 Received: date; Accepted: date; Published: date

10 **Abstract:** Lysenin, a pore forming toxin (PFT) extracted from *Eisenia fetida*, inserts
11 voltage-regulated channels into artificial lipid membranes containing sphingomyelin. The
12 voltage-induced gating leads to a strong static hysteresis in conductance, which endows lysenin
13 with molecular memory capabilities. To explain this history-dependent behavior we hypothesized
14 a gating mechanism that implies the movement of a voltage domain sensor from an aqueous
15 environment into the hydrophobic core of the membrane under the influence of an external electric
16 field. In this work, we employed electrophysiology approaches to investigate the effects of ionic
17 screening elicited by metal cations on the voltage-induced gating and hysteresis in conductance of
18 lysenin channels exposed to oscillatory voltage stimuli. Our experimental data show that screening
19 of the voltage sensor domain strongly affects the voltage regulation only during inactivation
20 (channel closing). In contrast, channel reactivation (reopening) presents a more stable, almost
21 invariant voltage dependency. Additionally, in the presence of anionic Adenosine 5'-triphosphate
22 (ATP), which binds at a different site in the channel's structure and occludes the conducting
23 pathway, both inactivation and reactivation pathways are significantly affected. Therefore, the
24 movement of the voltage domain sensor into a physically different environment that precludes
25 electrostatically bound ions may be an integral part of the gating mechanism.26 **Keywords:** lysenin; pore forming toxins; voltage gating; hysteresis; electrostatic screening27 **Key Contribution:** This study investigates the voltage regulation of the pore forming toxin lysenin
28 and proposes a gating mechanism that implies the movement of a voltage domain sensor from an
29 aqueous environment into the hydrophobic core of the membrane upon voltage-induced
30 conformational changes.

31

32

1. Introduction

33 Lysenin, a PFT found in the coelomic fluid of the red earthworm *E. fetida*, induces cytolysis and
34 hemolysis of cells that contain sphingomyelin in their plasmalemma [1-5]. Electrophysiology [2,6,7]
35 and atomic force microscopy [8-10] investigations of lysenin inserted into artificial membrane
36 systems have shown that this lytic activity stems from self-insertion of large conducting pores in the
37 target membrane. The physiological role of lysenin is still obscure; nonetheless, lysenin channels
38 possess a great variety of intricate biophysical properties which are commonly shared with ion
39 channels, including large transport rate and selectivity [2,7]. Additionally, lysenin is endowed with
40 unique regulatory mechanisms that set it apart from other PFTs. For example, when reconstituted in
41 artificial membrane systems, lysenin channels show reversible ligand-gating induced by multivalent
42 cations [11,12]. Remarkably, the ligand-induced gating is influenced by the charge density of the

43 ligands; small and highly charged ions (e.g., trivalent metal cations) bind the channel protein at a specific site and induce conformational changes that switch the channel's conductance between open (fully conducting) and closed (non-conducting), while divalent or voluminous polycations force the channel into a sub-conducting state [11,12]. The macroscopic conductance of the channels is also reversibly modulated by purines (e.g., adenosine phosphates), for which the mechanism of conductance reduction stems from anions binding to a specific site inside the channel's lumen and impeding the ionic flow [13]. This mechanism of channel occlusion is fundamentally different from ligand-induced gating, which employs a cation-binding site to induce conformational changes.

51 The most striking feature of lysenin channels is their unique voltage regulation, which has been
52 extensively explored in multiple studies [2,6,7,14,15]. Voltage regulation is a fundamental feature of
53 many PFTs, which generally present symmetrical voltage gating at large transmembrane potentials
54 [16]. In contrast, lysenin channels displays asymmetrical voltage induced gating, which occurs at
55 low transmembrane voltages [6,7] and resembles a basic feature of voltage-gated ion channels.
56 Specifically, lysenin channels are in a high-conductance state (open) for a large range of negative
57 voltages and at low positive voltages. At transmembrane potentials exceeding ~10-20 mV, the
58 lysenin channels transition to a closed conformation characterized by negligible conductance [6,17].

59 For a population of lysenin channels, the open-close transition is described by a Boltzmann
60 distribution within a two-state model for which the transition is relatively slow, being characterized
61 by a relaxation time of several seconds [17]. The slow response to applied voltages creates premises
62 for dynamic hysteresis in conductance which occur when applying variable voltages that change too
63 fast to be followed by conformational changes of the channels [18]. This non-equilibrium leads to
64 distinct pathways for channel inactivation (channel closing induced by increasing, ascending
65 voltage ramps) and reactivation (channel reopening during decreasing, descending voltage ramps).
66 Dynamic conductance hysteresis, which may be a source of molecular memory, is a fundamental
67 feature of voltage-gated ion channels exposed to oscillatory voltages for which the period of the
68 stimulus is comparable to the relaxation time [18]. However, this phenomenon fails to account for
69 the behavior of lysenin. Lysenin presents a large, static hysteresis in conductance [14,17], which is
70 not common among ion channels or pore forming proteins. While dynamic hysteresis vanishes
71 when the period of the voltage stimulus greatly exceeds the characteristic relaxation time (i.e., when
72 the channels are at equilibrium at any given time during voltage stimulation), lysenin channels
73 retain conductance hysteresis over voltage ramps lasting several hours [17], much larger than their
74 relaxation time.

75 This unusual feature may be related to the mechanism by which lysenin channels respond to
76 voltage stimuli. In experiments investigating the effects of temperature on lysenin gating [17], it has
77 been found that higher temperatures elicit a strong shift of the voltage-induced gating during
78 ascending voltage ramps. In contrast, temperature has negligible influence on channel reactivation
79 (descending voltage ramps) and the open probability (P_{open}) is invariant. This stable reactivation
80 pathway leads to a static hysteresis [17], which could be better understood by gaining more insights
81 into the gating mechanism. This may be possible by considering recent structural data of the lysenin
82 channels [19-21], which in conjunction with novel explorations may shed more light on lysenin's
83 intricate voltage-induced gating and molecular memory.

84 It has been suggested that lysenin channels alter their conformation by the movement of a gate
85 coupled to a charged voltage domain sensor when under the influence of an external electric field
86 [6], which is functionally similar to many voltage-gated ion channels [22-28]. Structural data reveals
87 the presence of hinge-like, flexible structures essential for pore formation [19-21] which may allow
88 the elusive voltage domain sensor to move. Since both ionic strength and pH strongly modulate the
89 voltage-induced gating of lysenin channels [6], it is natural to assume that the charged voltage
90 domain sensor is exposed to the bulk ionic solution at rest (the state in which all the channels are
91 open at zero transmembrane potential), and screened. To explain the invariant reactivation pathway,
92 we hypothesized that conformational changes, leading to channel closing, move the voltage domain
93 sensor into an environment for which novel physical properties influence how the channels will
94 further respond to voltage stimuli, such as the hydrophobic core of the membrane. Irrespective of

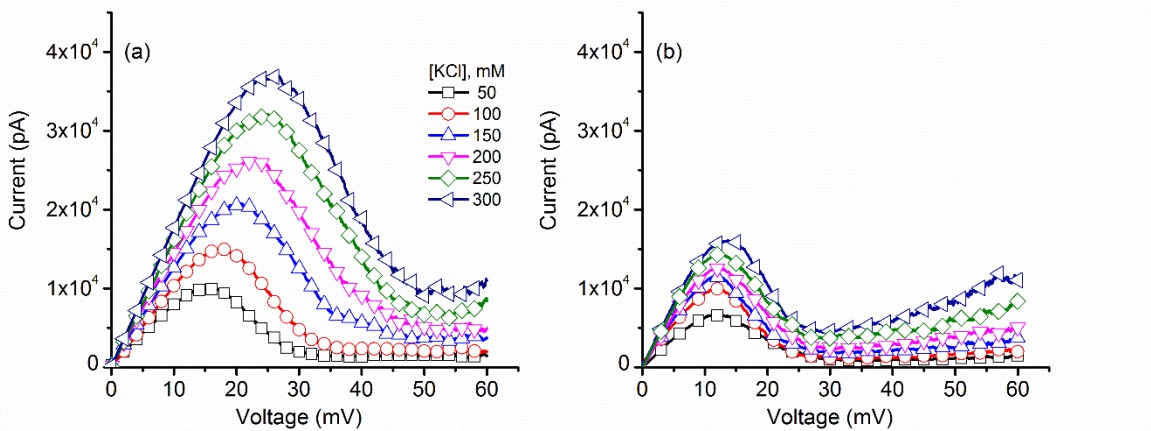
95 different nomenclatures used to define the protein domains, available X-ray and Cryo-EM structural
96 data [19,21], , show a mushroom-shaped channel comprising a head and a β -barrel long pore (stem).
97 One may surmise that the voltage domain sensor could be located in the head region since those
98 domains are more prone to movement. In addition, the same structural data indicates the presence
99 of multiple charged sites capable of binding both anions and cations, and lysenin presents such
100 capabilities [11-13,29].

101 The present work was undertaken to produce evidence for the hypothesis that the voltage
102 domain sensor moves into a physically different environment during gating. Our investigations
103 considered electrostatic screening elicited by monovalent and multivalent metal cations acting as
104 counterions for the voltage domain sensor. A simple two-state gating model that assumes a
105 Boltzmann distribution of the states [6,30-32] allowed us to estimate the midway voltage of
106 activation ($V_{0.5}$, the voltage at which the P_{open} equals 0.5) and the number n of elementary gating
107 charges in various experimental conditions comprising electrostatic screening induced by
108 counterions. Our results show that electrostatic screening has a major influence on channel
109 inactivation, while the reactivation pathway is basically invariant. However, investigations
110 conducted by employing ATP, which modulate the macroscopic conductance by binding to the
111 channel lumen and partially occluding the conducting pathway [13], show a quantitatively and
112 qualitatively different influence on voltage-induced gating, in support of the hypothesized gating
113 mechanism.

114 2. Results and Discussions

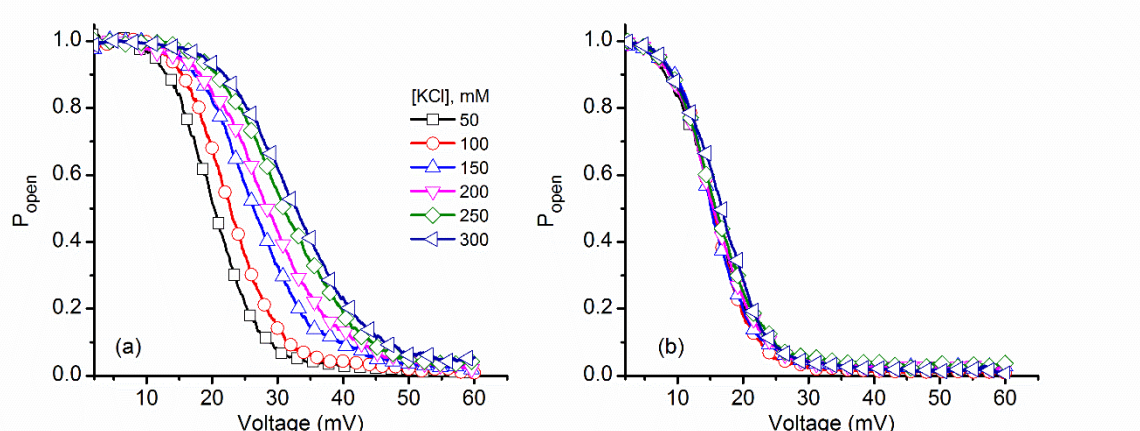
115 2.1. Monovalent metal cations modulate the voltage-induced gating of lysenin channels during inactivation, 116 while minimally influencing the reactivation pathway

117 The macroscopic ionic currents through a large population of lysenin channels, which were
118 inserted into the bilayer membrane and exposed to increasing monovalent ion concentrations,
119 underwent visible changes with regards to their magnitude and voltage required to initiate the
120 open-close transitions during ascending voltage ramps (channel closing, or inactivation, Figure 1a),
121 as our group reported in a previous study [6]. Addition of KCl yielded larger slopes of the linear
122 portion of the current-voltage (I-V) curves recorded at low voltages (i.e., a larger macroscopic
123 conductance, equal to I/V), which follows the increase of the support electrolyte's ionic conductivity.
124 In addition, we observed a significant shift in the voltage required to initiate voltage-induced gating,
125 which was also dependent on the ionic concentration of the bulk [6]. This shift suggests that the
126 voltage domain sensor of the channel was exposed to the external ionic solution and addition of
127 counterions enhanced electrostatic screening and reduced the gating charge. Consequently, larger
128 transmembrane voltages and electric fields were required to actuate the gate and close the channel.
129 In contrast, the ionic currents recorded for descending voltage ramps (channel reopening, or
130 reactivation, after voltage-induced closing) show both a different qualitative and quantitative
131 response to monovalent ion addition (Fig. 1b). To facilitate direct comparison with the ionic currents
132 recorded during ascending ramps, an identical range for the y axis was used to plot the I-V
133 characteristic corresponding to descending voltage ramps. For identical ionic concentrations, the
134 maximal currents recorded during the descending ramps are clearly smaller than what was recorded
135 for the ascending ramps, demonstrating the previously observed hysteresis in conductance [14,17].
136 In brief, for the same transmembrane voltage, the macroscopic current may have different values
137 depending on the channel's history (previously open, or previously closed, respectively).
138 Nonetheless, when the decreasing transmembrane voltages approached ~ 10 mV, the channels fully
139 reopened and their initial conductance was fully reinstated; as inferred from the I-V plots recorded
140 at low transmembrane voltages for all ionic concentrations and ramp directions, the currents and the
141 slopes of the I-V plots at low transmembrane potentials were identical for the two cases, indicating
142 full channel reopening. However, unlike what was observed for ascending voltage ramps,
143 monovalent cation addition did not significantly alter the voltage at which the close-open transition
144 occurred during descending ramps, irrespective of the ionic concentration.



145
146 **Figure 1.** Effects of KCl addition on the I-V characteristics of a population of lysenin channels. (a)
147 The I-V plots recorded during ascending voltage ramps indicated changes of the macroscopic
148 conductance (I/V) and voltage required to initiate gating. (b) The I-V plots corresponding to
149 descending voltage ramps showed similar changes in the macroscopic conductance of open channels
150 but less dependence of the close-open transition on the ionic concentration, along with hysteresis in
151 macroscopic conductance. Each trace in the panels represents a single, typical run for each particular
152 concentration. All the points in the plots are experimental points; the symbols have been added as a
153 visual aid to discriminate between ionic concentrations.

154 These differences in response to applied voltages, ramp direction and ionic conditions were also
155 observed in the experimental P_{open} plots (Figure 2), constructed as described in the Materials and
156 Methods section. The very low-voltage experimental points presented large deviations of the P_{open}
157 (due to the very low currents and large noise, which may imply division by near zero numbers), and
158 these points were not represented in the plots. KCl addition yielded a significant rightward shift of
159 the P_{open} for ascending voltage ramps (Figure 2a), while only minor changes were observed for the
160 descending voltage ramps (Figure 2b). These results show a steady, almost invariant channel
161 reactivation pathway, resembling what our group has reported in experiments exploring the effects
162 of temperature on lysenin channel voltage-induced gating [17].

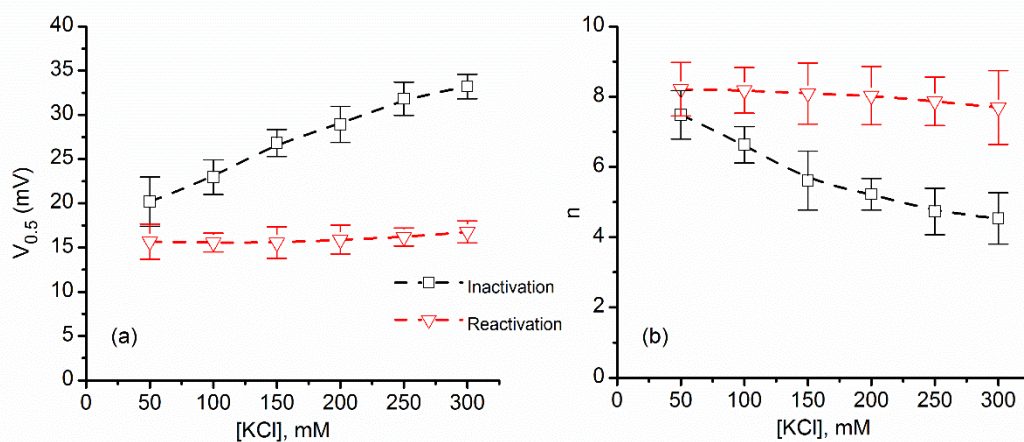


163
164 **Figure 2.** KCl influence on lysenin channels' experimental open probability. (a) The open
165 probability of lysenin channels as a function of voltage underwent a substantial rightward shift for
166 the ascending voltage ramps as the KCl concentration increased. (b) In contrast, negligible changes of
167 the open probability occurred during channel reactivation (descending voltage ramps), irrespective
168 of the bulk KCl concentration. Each plot represents a typical curve of the experimental open

169 probability calculated for each particular concentration. All the points in the plots are experimental
 170 points, with the symbols added to allow identification of the ionic conditions.

171 For both ramps, we estimated the midway voltage of activation, $V_{0.5}$, from the P_{open} plots [31,33].
 172 Figure 3a shows that $V_{0.5}$ increased monotonically from ~20 mV to ~35 mV upon KCl addition during
 173 ascending voltage ramps. As we already surmised from the P_{open} plots, only negligible changes of
 174 $V_{0.5}$ were observed for the descending voltage ramps. The $V_{0.5}$ values were next introduced into the
 175 Boltzmann distribution equation (see Materials and Methods: Equation 2) to calculate the number of
 176 elementary gating charges n (depicted in Figure 3b).
 177

178 As predicted from the channel inactivation P_{open} plots, monovalent ion addition led to major
 179 variation of the gating charge, which decreased with increasing ionic strength from ~7.5 e to ~4.5 e;
 180 the non-linear decrease resembles an exponential decay, in accordance with surface screening [34].
 181 However, the descending voltage ramps yielded a much smaller variation of the gating charge, and
 182 were slightly greater (up to ~8 e) for all experimental ionic strengths.



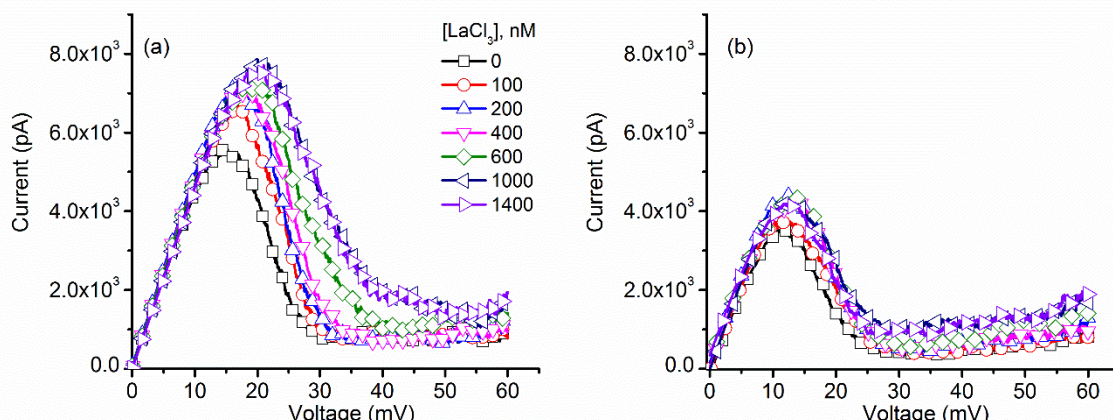
183 **Figure 3.** Variation of the midway voltage of activation $V_{0.5}$ and number of elementary gating
 184 charges n as a function of KCl concentration. (a) The experimental values of $V_{0.5}$ calculated for
 185 ascending voltage ramps presented a significant increase with added KCl, while only a weak
 186 influence was encountered for descending voltage ramps. (b) The values of n calculated from the fit
 187 of the Boltzmann distribution equation, for each KCl concentration, suggested strong electrostatic
 188 screening of the voltage domain sensor for channel inactivation; only minor changes were estimated
 189 for channel reactivation. Each experimental point is represented as mean \pm SD from three
 190 independent experiments.

191 These intricate results show that the history of channel conformation (i.e., closed or open state)
 192 influences its further response to applied voltages, which is the essence of molecular memory [17].
 193 This may be realized by dynamic changes in the energy landscape elicited upon conformational
 194 changes. The more stable, almost invariant reactivation pathway may provide some clues for
 195 understanding the mechanism of the gating process. The strong influence of ionic strength on the
 196 gating charge estimated for the inactivation pathway, together with the minimal influence observed
 197 during reactivation, suggests that the voltage domain sensor may be exposed to very different
 198 environmental conditions during transitions. For a channel in the open state, the voltage domain
 199 sensor appears to be exposed to the external electrolyte solution. Therefore, KCl addition promoted
 200 electrostatic screening of the gating charge, which led to the rightward shift of the P_{open} during the
 201 ascending voltage ramps in a concentration-dependent manner. Channel closure is accompanied by
 202 conformational changes and movement of the voltage domain sensor that acts on the gate. This
 203 process may result in positioning of the voltage domain sensor into a low polarity environment (i.e.,
 204 the hydrophobic core of the membrane), from which both water and bound counterions are
 205 excluded by the large Born energy penalty [35–38]. Therefore, irrespective of the ionic strength, the

206 voltage domain sensor will be mostly stripped of electrostatically bound counterions upon gating.
 207 Consequently, after channel closing, the voltage domain sensor is characterized by a larger gating
 208 charge less influenced by the ionic strength of the bulk solution, which may explain the more stable
 209 reopening (reactivation) pathway. This proposed mechanism is well-established for ion channels, for
 210 which the movement of a charged voltage domain sensor into the hydrophobic core of the bilayer
 211 has been reported [39–43]. Therefore, the “paddle in oil” concept, which consists of large movements
 212 of the voltage domain sensor into the hydrophobic core of the membrane [41], is accepted as a valid
 213 model of ion channel gating.

214 *2.2. Multivalent metal cations influence the voltage regulation of lysenin channels similarly to monovalent ions*

215 Electrostatic screening is dependent on ionic strength, which increases with the second power
 216 of the electrovalence [44,45], and thus one may expect an even greater influence on the channel’s
 217 response upon exposure to multivalent ions. However, our group has reported that multivalent ions
 218 induce channel closure by a ligand-induced gating mechanism [11,12], which may introduce
 219 roadblocks for such investigations. For example, trivalent metal cations (especially lanthanides)
 220 reversibly close lysenin channels and annihilate their macroscopic conductance at $\sim 100 \mu\text{M}$ bulk
 221 concentration [11,12]. Although μmolar addition of La^{3+} may elicit only minor changes of the
 222 macroscopic conductance, such small concentrations may not sufficiently screen a gating charge
 223 which is simultaneously exposed to substantially larger concentrations of monovalent ions in the
 224 support electrolyte. However, it appears that the binding of multivalent ions is more specific and
 225 much stronger than monovalent ions [11,12]. This may aid in achieving significant changes of the
 226 gating charge without major changes of the macroscopic conductance (owing to significant
 227 ligand-induced gating), even upon simultaneous exposure to relatively high concentrations of
 228 monovalent ions. Therefore, we investigated the effects of La^{3+} ions on the voltage gating of lysenin
 229 channels while using the same experimental approaches adopted for KCl. Addition of small
 230 amounts of La^{3+} (no more than $2 \mu\text{L}$ of various stock LaCl_3 solutions with concentration in the range
 231 $0.1 \text{ mM} - 1 \text{ mM}$ for each addition) to the bulk electrolyte (1 mL of 100 mM KCl) to achieve target La^{3+}
 232 concentrations (up to $1.4 \mu\text{M}$) elicited great changes in the I-V characteristics plotted for ascending
 233 voltage ramps (Figure 4a). As we observed for the case of KCl, La^{3+} addition required greater
 234 transmembrane voltages to initiate voltage-induced gating. For all the La^{3+} concentrations used in
 235 these experiments, almost identical slopes of the I-V curves at low transmembrane potentials (the
 236 linear, ohmic portion of the curves) indicated that La^{3+} addition elicited negligible changes with
 237 respect to the solution conductivity or ligand-induced gating. Comparative analysis of the I-V curves
 238 (Figure 4) revealed that, similar to KCl, the voltage required for reopening the channels during
 239 descending voltage ramps was smaller than what was required for closing, and that the reopening
 240 occurred at similar voltages irrespective of the amount of added La^{3+} .

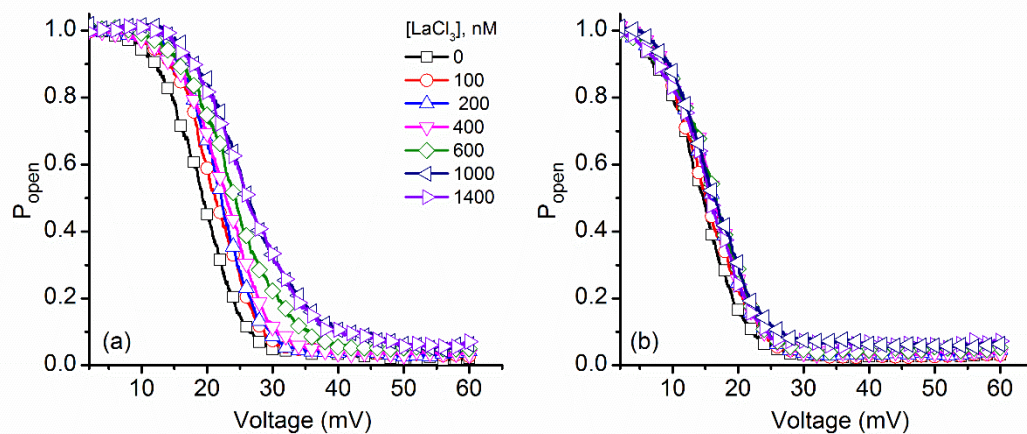


241

242 **Figure 4.** LaCl_3 influence on the I-V characteristics of lysenin channels. (a) The I-V plots recorded for
 243 ascending voltage ramps indicated LaCl_3 induced changes of the voltage required to initiate gating.

244 (b) The I-V plots corresponding to descending voltage ramps indicated a minimal influence from the
 245 multivalent cations. Each trace in the plots for both panels represents experimental points, with the
 246 symbols added as a visual aid.

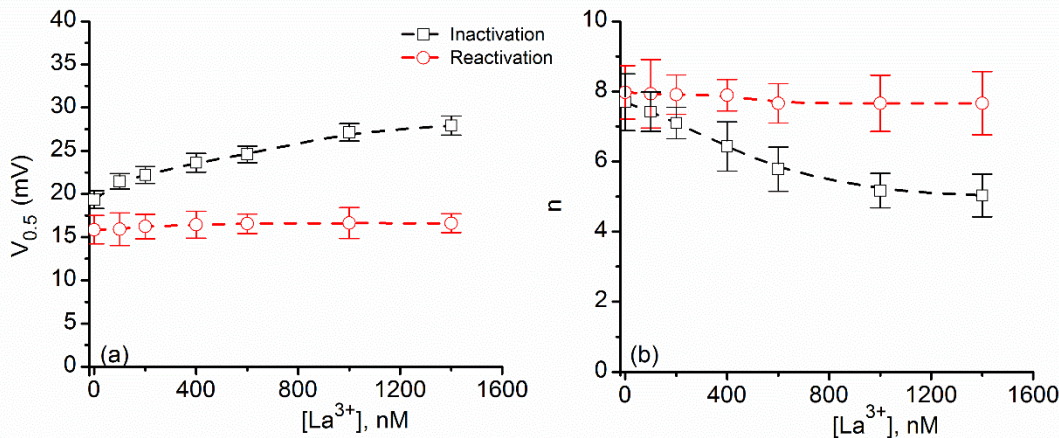
247 These features were also observed in the experimental P_{open} plots constructed for both
 248 ascending and descending voltage ramps recorded upon La^{3+} addition (Figure 5). The multivalent
 249 metal cations induced a significant rightward shift of the P_{open} for ascending voltage ramps, while
 250 the effects presented by the same ions on the P_{open} corresponding to descending voltage ramps were
 251 minimal. Therefore, we concluded that the reactivation pathway suffered little influence from the
 252 multivalent ions and maintained invariance. In addition, these experimental data show that the
 253 influence of La^{3+} manifests even in the presence of much larger concentrations of monovalent ions in
 254 the bulk solution, suggesting a greater affinity for their binding sites. We concluded that both
 255 monovalent and multivalent cations may compete for the same binding sites since counterion
 256 binding is greatly diminished in the presence of very large concentrations of monovalent cations
 257 [13].



258

259 **Figure 5.** Changes of the experimental open probability (P_{open}) of lysenin channels induced by
 260 addition of LaCl_3 . (a) The voltage-dependent open probability of the lysenin channels shifted
 261 substantially rightward for the ascending voltage ramps as the LaCl_3 concentration increased. (b)
 262 Conversely, and as with addition of KCl, minor changes were observed during descending voltage
 263 ramps. Each trace was constructed from experimental points, with the symbols added for better
 264 discrimination between ionic conditions.

265 The experimental $V_{0.5}$ (Figure 6a) and n (Figure 6b) estimated from the best fit of the P_{open} curves
 266 for ascending voltage ramps increased significantly (from ~ 18 mV to ~ 26 mV) upon sub- μ molar La^{3+}
 267 addition, showing great screening effectiveness compared to KCl. Such result was expected, based
 268 on the assumption that both monovalent and multivalent cations elicit ionic screening. Nonetheless,
 269 steadier values of $V_{0.5}$ and n were obtained during descending voltage ramps, similar to KCl. This
 270 constitutes supplementary evidence for a gating mechanism that implies the movement of the
 271 voltage domain sensor into a more hydrophobic environment and supports the hypothesis that
 272 multivalent and monovalent cations act similarly, but with different affinities with respect to
 273 electrostatic binding to the voltage domain sensor.



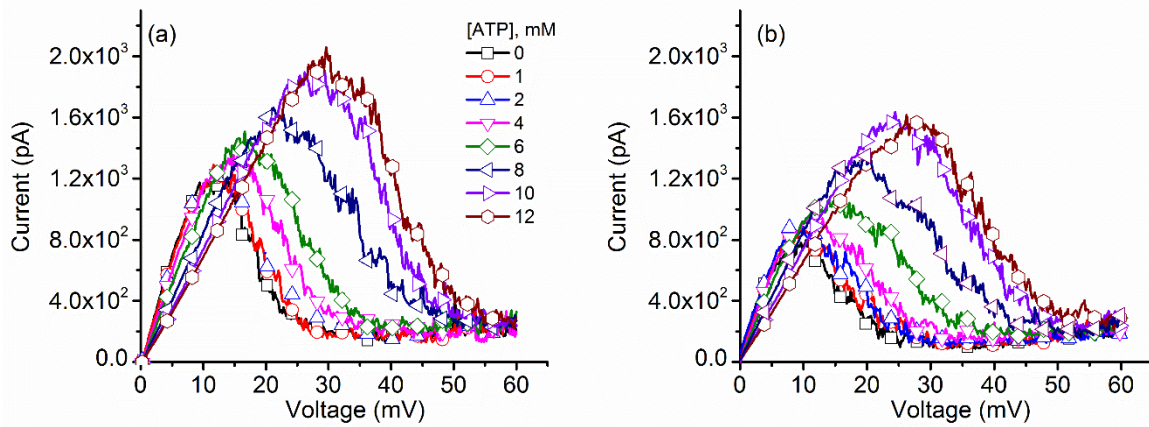
274

275 **Figure 6.** The dependence of $V_{0.5}$ and n on the bulk LaCl_3 concentration. (a) Addition of LaCl_3
 276 induced significant increases of the $V_{0.5}$ calculated for ascending voltage ramps, while having yielded
 277 little change for the descending voltage ramps. (b) The total number of elementary charges indicated
 278 effective electrostatic screening of the voltage domain sensor upon addition of LaCl_3 during channel
 279 inactivation, while insignificant changes occurred during reactivation. Each experimental point is
 280 represented as mean \pm SD from three independent experiments.

281 2.3. ATP binding to lysenin channels modulates the voltage-induced gating and affects both the inactivation
 282 and reactivation pathways

283 The above experiments comprised addition of cations capable of electrostatic interactions with
 284 the voltage domain sensor, hence eliciting ionic screening of the gating charge. However, lysenin
 285 channels are also capable of interacting with large anions, such as adenosine phosphates, whose
 286 interaction manifests as changes in the macroscopic conductance in a concentration dependent
 287 manner [13]. Unlike multivalent cations, which most probably bind to a negatively charged site on
 288 the voltage domain sensor, purines most likely bind a positively-charged region in channel lumen
 289 and elicit physical occlusion of the conducting pathway. Moreover, the binding of purines is a
 290 cooperative process, and is most prominent for the highly charged ATP [13]. Therefore, we
 291 questioned whether ATP binding to a different site may have a similar influence on the voltage
 292 gating profile of lysenin channels, which would challenge the movement of the voltage domain
 293 sensor into a more hydrophobic environment as a valid hypothesis.

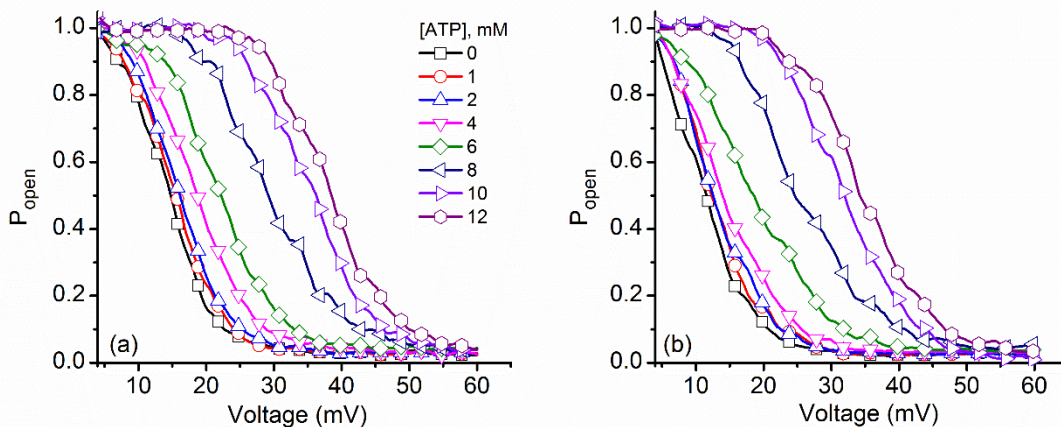
294 To answer these questions, we investigated the effects of ATP addition on the lysenin channel
 295 voltage-induced gating in similar experiments comprised of ascending and descending voltage
 296 ramps. The experimental I-V plots (Figure 7) show that ATP addition to the 135 mM KCl bulk
 297 slightly decreased the macroscopic conductance of the open channels in a concentration dependent
 298 manner [13], as indicated by the reduced slopes of the linear portions of the I-V curves at low
 299 voltages. ATP addition induced a significant shift of the voltage required to close the channels
 300 during ascending voltage ramps, similar to monovalent and multivalent metal cations. The response
 301 to voltage in the presence of ATP recorded for descending voltage ramps (Figure 7b) was
 302 fundamentally different. The hysteresis in conductance remained, and manifested as a different,
 303 history-dependent macroscopic current recorded at identical transmembrane voltages. However,
 304 the reactivation pathway in the presence of ATP was not invariant, as concluded from the changes
 305 observed in the I-V plots.



306

307 **Figure 7.** ATP affects the I-V characteristics of lysenin channels in a concentration dependent
 308 manner. (a) The I-V plots recorded during ascending voltage ramps showed that ATP addition
 309 modulated the macroscopic conductance and voltage-induced gating of lysenin channels. (b)
 310 Opposite to metal cations, ATP induced similar significant changes during descending voltage
 311 ramps. Each trace in the panels of the plots represents experimental points, and the symbols have
 312 been added to allow easy identification of experimental concentrations.

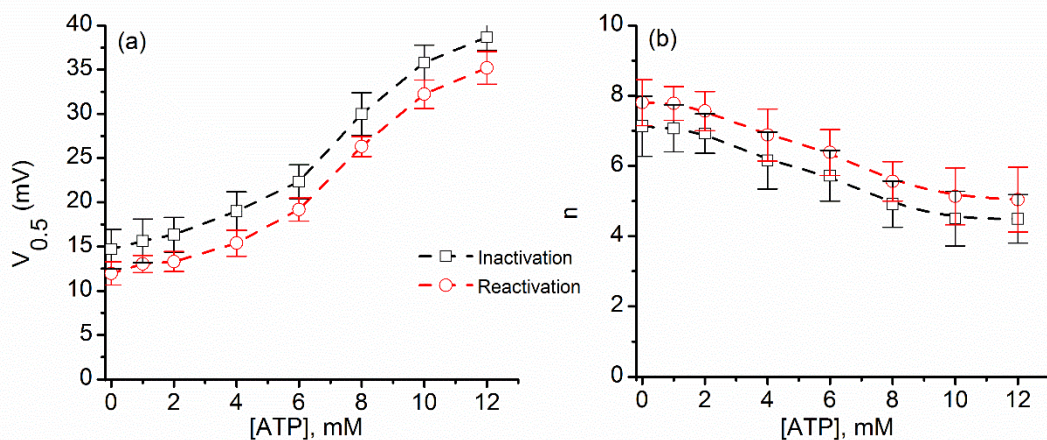
313 These features are better observed in the experimental P_{open} curves (Figure 8), which were
 314 devoid of any influence from the changes in the macroscopic conductance of open channels. Channel
 315 inactivation during ascending voltage ramps show a strong rightward shift with ATP addition
 316 (Figure 8a), similar to what was observed for both monovalent and multivalent cations. What is
 317 striking is that the P_{open} for descending voltage ramps presented a significant
 318 concentration-dependent rightward shift (Figure 8b), which is very different from the invariant
 319 curves recorded for metal cation addition. Moreover, both I-V and P_{open} plots suggested that a
 320 maximal influence of ATP manifests in the 4 mM – 10 mM concentration range, while outside this
 321 range the induced changes were smaller. This is consistent with the cooperative binding of ATP to
 322 lysenin channels, as described in a previous report [13].



323

324 **Figure 8.** Increased ATP concentration shifted the voltage-dependent open probability of lysenin
 325 channels. Addition of ATP induced a rightward shift of the experimental open probability during
 326 both (a) ascending and (b) descending voltage ramps. Each plot represents a typical curve of the
 327 experimental open probability calculated for each particular concentration. All the points in the plots
 328 are experimental points, and the symbols have been added to allow easy identification of the ATP
 329 concentrations. For representation, the P_{open} curves have been smoothed with the Savitsky-Golay
 330 protocol (23 smoothing points).

331 Differences between metal cations and ATP were also observed in the estimated $V_{0.5}$ and n
 332 calculated at different concentrations (Figure 9). Both $V_{0.5}$ and n followed similar patterns of change
 333 with ATP concentration, as expected from the summary analysis of the P_{open} and I-V plots. Also, the
 334 particular sigmoidal shape of the plots is in agreement with the cooperative binding of ATP to
 335 lysenin [13]. Interestingly, the $V_{0.5}$ value measured at 0 mM ATP (i.e., ~12 mV) was the smallest
 336 recorded from all the experiments described in this work. This may be explained by considering the
 337 consistently lower number of channels inserted in the membrane for the ATP experiments; previous
 338 studies reported that crowding in the membrane plane (achievable at large channel densities) may
 339 influence the voltage gating of lysenin channels [15]. In the case of the ATP experiments, a different
 340 lysenin batch was used, which consistently provided a lower number of inserted channels that gated
 341 at lower transmembrane voltages.



342

343 **Figure 9.** ATP addition alters $V_{0.5}$ and n for both inactivation and reactivation voltage ramps. For the
 344 ascending and descending voltage ramps, both $V_{0.5}$ (a) and n (b) varied with the concentration of
 345 ATP. Each experimental point is represented as mean \pm SD from three independent experiments.

346 We presented evidence in support of the hypothesis that the voltage domain sensor of the
 347 lysenin channel moves into a different physical environment upon voltage-induced gating. Based on
 348 earlier evidence presented for ion channels, we assumed that the gating charge, exposed to the
 349 aqueous environment at rest, may penetrate deep into the membrane and exclude the bound ions.
 350 Before closing, the voltage domain sensor is electrostatically screened by cations; therefore, ionic
 351 strengths significantly modulate the voltage-induced gating. Channel reopening after closing
 352 comprises a voltage domain sensor which is minimally screened and results in a more stable
 353 reactivation pathway. From investigating the influence of ATP on voltage gating, we concluded that
 354 anions act in a very different manner than cations because they do not bind to the same sites of the
 355 channel. The cations bind to the voltage domain sensor, which then undergoes conformational
 356 changes and penetrates into a more hydrophobic environment from which water and ions are
 357 excluded. For ATP, which binds a different site, the influence on the voltage induced gating may be
 358 explained by long range electrostatic interactions between the bound anions and the voltage domain
 359 sensor, which may manifest even when the voltage domain sensor is in a nonpolar environment. The
 360 proposed gating mechanism is supported by experimental data but we may not overlook some
 361 experimental and theoretical limitations. In this work we consistently used a reasonably-long period
 362 for the driving voltage stimulus (20 minutes), which is much larger than the characteristic relaxation
 363 time of lysenin channels (seconds). However, addition of cations or anions may substantially change
 364 the relaxation time, and therefore the I-V and P_{open} plots may not represent true steady states.
 365 Nonetheless, in such situations, the channels that closed at lower voltages resided for longer times in
 366 the closed state, yet the reactivation pathway was invariant. Also, the Boltzmann distribution
 367 considered in this work (and similar approaches [31]) did not account for dynamic changes of the
 368 energy landscape during gating. In spite of these limitations, both the similarities and differences
 369 between the voltage-induced gating of lysenin channels exposed to cations and anions support a

370 model in which the voltage domain sensor moves into the membrane, and may explain the
371 persistent hysteresis in conductance.

372 3. Materials and Methods

373 3.1. Bilayer lipid formation, channel insertion, and ionic addition

374 The vertical bilayer membrane chamber consisted of two polytetrafluoroethylene (PTFE)
375 reservoirs (~ 1 mL volume each) separated by a thin PTFE film in which a small hole (~ 70 μ m
376 diameter) was pierced by an electric spark. The reservoirs were filled with electrolyte solutions (50
377 mM KCl, if not otherwise noted, buffered with 20 mM HEPES, pH 7.2) and connected to the
378 Axopatch 200B electrophysiology amplifier (Molecular Devices) via Ag/AgCl electrodes. The analog
379 signal of the amplifier was further digitized and recorded with the DigiData 1440A digitizer
380 controlled by the pClamp 10.2 software package (Molecular Devices). The bilayer was produced
381 using a mixture of 1 mg asolectin (Sigma-Aldrich), 0.4 mg cholesterol (Sigma-Aldrich), and 0.5 mg
382 sphingomyelin (AvantiLipids) in 100 μ L n-decane (TCI America). The bilayer integrity was verified
383 by both capacitance and conductance measurements. Channel insertion was performed by addition
384 of small amounts of lysenin (0.3 pM final concentration, Sigma-Aldrich) to the ground reservoir
385 under continuous stirring with a low noise magnetic stirrer (Warner Instruments). Individual
386 channel insertion was monitored by observing the discrete, step-wise changes of the ionic current
387 through the membrane biased by -60 mV transmembrane potentials [7]. After completion of
388 insertion, observed as a steady value of the ionic current, the free lysenin was removed by flushing
389 the ground reservoir with fresh buffered electrolyte. Lysenin gating at positive potentials was
390 observed from I-V plots recorded in the range 0 mV: +60 mV by exposing the channel-containing
391 membrane to voltage ramps created with the digitizer. We observed that different batches of lysenin
392 presented slight differences with respect to voltage-induced gating (i.e. variations of the voltage
393 required to initiate gating), therefore we used identical batches of lysenin for each independent
394 experiment focused on investigating the influence of a particular ion on the gating profile.

395 Stock solutions of KCl (Fisher Scientific), LaCl₃ (Alpha Aesar), and ATP (Sigma-Aldrich) were
396 prepared by dissolving the powders in 20 mM HEPES (pH 7.2). To achieve the target concentrations
397 in the bulk, corresponding amounts of stock solutions were added to both reservoirs under
398 continuous stirring. This procedure was repeated for all target concentrations achieved for the
399 experiments.

400 3.2. Data collection, analysis, and mathematical modelling

401 For each ionic concentration, the voltage-induced gating of lysenin channels was investigated
402 by recording the ionic currents in response to linear, triangle-shaped voltage ramps. The ramps were
403 created with the pClamp 10.2 software package and delivered to the electrophysiology amplifier via
404 one of the digitizer's outputs. Each voltage ramp stimulus had a period of 20 minutes (10 minutes for
405 ascending, and 10 minutes for descending) in the range 0 mV: +60 mV, at a sampling rate of
406 minimum 1 second, with a 1 kHz hardware filter. Each recording was saved as a separate file and
407 further analyzed with Origin 8.5.1 (OriginLab), pClamp 10.2 and Mathematica 10.4 (Wolfram
408 Research).

409 For analysis and modelling, we considered that the voltage-induced gating of lysenin channels
410 is described by a two-state model [6]:

$$Open \leftrightarrow Closed \quad (1)$$

412 Within this model, the open probability P_{open} of the channels in response to applied voltages is
413 described by the Boltzmann distribution [31,46]:

414

$$P_{open} = \frac{1}{1 + e^{-\frac{neF(V_{0.5} - V)}{RT}}}, \quad (2)$$

415 where n is the total number of elementary gating charges e of the voltage domain sensor ($e =$
 416 1.6×10^{-19} C), $V_{0.5}$ is the midway voltage of activation (the voltage at which $P_{open} = 0.5$), V is the
 417 applied voltage, R is the universal gas constant (8.34 J/K), F is Faraday's number ($F = 96485.33$
 418 C/mol), and T is the absolute temperature ($T = 295$ K).

419 Within the two-state model, the experimental open probability for each applied voltage was
 420 derived from [23,32,47]:

421

$$P_{open}(V) = \frac{I}{I_{max}}, \quad (3)$$

422 where I is the ionic current measured for a particular voltage, and I_{max} is the ionic current that
 423 would be recorded at the same voltage if all the channels were open. For each particular voltage, I_{max}
 424 was estimated from a straight line constructed by fitting the linear portion of each I-V curve
 425 recorded at low transmembrane voltages (when all the channels are open).

426 The midway voltage of activation was experimentally determined from the P_{open} , plotted for
 427 each of the ionic conditions, and further used in the theoretical model to determine n . Since even a
 428 closed lysenin channel may present a small leakage current [6,17], this was corrected in the
 429 experimental P_{open} only for the two highest KCl concentrations used in our experiment, which
 430 presented visible leakages. No other correction was performed for experimental data. All graphs
 431 have been prepared using the Origin 8.5.1 software.

432

433 Author Contributions: "Conceptualization, S.L.B and D.F.; Methodology, S.L.B., C.A.T, and D.F.; Software,
 434 T.C., K.S.W, and D.F.; All the authors contributed to data recording, analysis, interpretation, and manuscript
 preparation.

435

436 Funding: This research was funded by National Science Foundation (NSF, USA) grant number 1554166 and
 National Aeronautics and Space Administration (NASA, USA) grant number NNX15AU64H.

437

438 Conflicts of Interest: The authors declare no conflict of interest. The funders had no role in the design of the
 439 study; in the collection, analyses, or interpretation of data; in the writing of the manuscript, and in the decision
 to publish the results.

440

441 References

442

1. Bruhn, H.; Winkelmann, J.; Andersen, C.; Andra, J.; Leippe, M. Dissection of the mechanisms of cytolytic and antibacterial activity of lysenin, a defense protein of the annelid Eisenia fetida. *Developmental and Comparative Immunology* **2006**, *30*, 597-606. DOI: 10.1016/j.dci.2005.09.002
2. Kwiatkowska, K.; Hordejuk, R.; Szymczyk, P.; Kulma, M.; Abdel-Shakor, A.-B.; Plucienniczak, A.; Dolowy, K.; Szewczyk, A.; Sobota, A. Lysenin-His, a sphingomyelin-recognizing toxin, requires tryptophan 20 for cation-selective channel assembly but not for membrane binding. *Molecular Membrane Biology* **2007**, *24*, 121-134. DOI: 10.1080/09687860600995540
3. Shakor, A.-B.A.; Czurylo, E.A.; Sobota, A. Lysenin, a unique sphingomyelin-binding protein. *FEBS Letters* **2003**, *542*, 1-6. DOI: 10.1016/S0014-5793(03)00330-2
4. Shogomori, H.; Kobayashi, T. Lysenin: A sphingomyelin specific pore-forming toxin. *Biochimica et Biophysica Acta* **2008**, *1780*, 612-618. DOI: 10.1016/j.bbagen.2007.09.001
5. Yamaji-Hasegawa, A.; Makino, A.; Baba, T.; Senoh, Y.; Kimura-Suda, H.; Sato, S.B.; Terada, N.; Ohno, S.; Kiyokawa, E.; Umeda, M., et al. Oligomerization and pore formation of a sphingomyelin-specific toxin, lysenin. *Journal of Biological Chemistry* **2003**, *278*, 22762-22770. DOI: 10.1074/jbc.M213209200

456 6. Fologea, D.; Krueger, E.; Lee, R.; Naglak, M.; Mazur, Y.; Henry, R.; Salamo, G. Controlled gating of
457 lysenin pores. *Biophysical Chemistry* **2010**, *146*, 25–29. DOI: 10.1016/j.bpc.2009.09.014

458 7. Ide, T.; Aoki, T.; Takeuchi, Y.; Yanagida, T. Lysenin forms a voltage-dependent channel in artificial
459 lipid bilayer membranes. *Biochemical and Biophysical Research Communications* **2006**, *346*, 288–292. DOI:
460 10.1016/j.bbrc.2006.05.115

461 8. Yilmaz, N.; Kobayashi, T. Visualization of lipid membrane reorganization induced by a pore-forming
462 toxin using high-speed atomic force microscopy. *ACS Nano* **2015**, *9*, 7960–7967. DOI:
463 10.1021/acsnano.5b01041

464 9. Yilmaz, N.; Yamada, T.; Greimel, P.; Uchihashi, T.; Ando, T.; Kobayashi, T. Real-time visualization of
465 assembling of a sphingomyelin-specific toxin on planar lipid membranes. *Biophysical Journal* **2013**,
466 *105*, 1397–1405. DOI: 10.1016/j.bpj.2013.07.052

467 10. Yilmaz, N.; Yamaji-Hasegawa, A.; Hullin-Matsuda, F.; Kobayashi, T. Molecular mechanisms of
468 action of sphingomyelin-specific pore-forming toxin, lysenin. *Seminars in Cell & Developmental Biology*
469 **2018**, *73*, 188–198. DOI: 10.1016/j.semcdb.2017.07.036

470 11. Fologea, D.; Al Faori, R.; Krueger, E.; Mazur, Y.I.; Kern, M.; Williams, M.; Mortazavi, A.; Henry, R.;
471 Salamo, G.J. Potential analytical applications of lysenin channels for detection of multivalent ions.
472 *Analytical and Bioanalytical Chemistry* **2011**, *401*, 1871–1879. DOI: 10.1007/s00216-011-5277-8

473 12. Fologea, D.; Krueger, E.; Al Faori, R.; Lee, R.; Mazur, Y.I.; Henry, R.; Arnold, M.; Salamo, G.J.
474 Multivalent ions control the transport through lysenin channels. *Biophysical Chemistry* **2010**, *152*,
475 40–45. DOI: 10.1016/j.bpc.2010.07.004

476 13. Bryant, S.; Shrestha, N.; Carnig, P.; Kosydar, S.; Belzeski, P.; Hanna, C.; Fologea, D. Purinergic control
477 of lysenin's transport and voltage-gating properties. *Purinergic Signalling* **2016**, *12*, 1–11. DOI:
478 10.1007/s11302-016-9520-9

479 14. Krueger, E.; Al Faouri, R.; Fologea, D.; Henry, R.; Straub, D.; Salamo, G. A model for the hysteresis
480 observed in gating of lysenin channels. *Biophysical Chemistry* **2013**, *184*, 126–130. DOI:
481 10.1016/j.bpc.2013.09.001

482 15. Krueger, E.; Bryant, S.; Shrestha, N.; Clark, T.; Hanna, C.; Pink, D.; Fologea, D. Intramembrane
483 congestion effects on lysenin channel voltage-induced gating. *European Biophysics Journal* **2016**, *45*,
484 187–194. DOI: 10.1007/s00249-015-1104-z

485 16. Bainbridge, G.; Gokce, I.; Lakey, J.H. Voltage gating is a fundamental feature of porin and toxin
486 β -barrel membrane channels. *FEBS Letters* **1998**, *431*, 305–308. DOI: 10.1016/S0014-5793(98)00761-3

487 17. Fologea, D.; Krueger, E.; Mazur, Y.I.; Stith, C.; Okuyama, Y.; Henry, R.; Salamo, G.J. Bi-stability,
488 hysteresis, and memory of voltage-gated lysenin channels. *Biochimica et Biophysica Acta -
489 Biomembranes* **2011**, *1808*, 2933–2939. DOI: 10.1016/j.bbamem.2011.09.005

490 18. Pustovoit, M.A.; Berezhkovskii, A.M.; Bezrukov, S.M. Analytical theory of hysteresis in ion channels:
491 Two state model. *Journal of Chemical Physics* **2006**, *125*, 194907. DOI: 10.1063/1.2364898

492 19. Bokori-Brown, M.; Martin, T.G.; Naylor, C.E.; Basak, A.K.; Titball, R.W.; Savva, C.G. Cryo-EM
493 structure of lysenin pore elucidates membrane insertion by an aerolysin family protein. *Nature
494 Communications* **2016**, *7*, 11293. DOI: 10.1038/ncomms11293

495 20. De Colibus, L.; Sonnen, A.F.; Morris, K.J.; Siebert, C.A.; Abrusci, P.; Plitzko, J.; Hodnik, V.; Leippe,
496 M.; Volpi, E.; Anderluh, G., et al. Structures of lysenin reveal a shared evolutionary origin for
497 pore-forming proteins and its mode of sphingomyelin recognition. *Structure* **2012**, *20*, 1498–1507.
498 DOI: 10.1016/j.str.2012.06.011

499 21. Podobnik, M.; Savory, P.; Rojko, N.; Kisovec, M.; Wood, N.; Hambley, R.; Pugh, J.; Wallace, E.J.;
500 McNeill, L.; Bruce, M., et al. Crystal structure of an invertebrate cytolysin pore reveals unique
501 properties and mechanism of assembly. *Nature Communications* **2016**, *7*, DOI: 11598.
502 10.1038/ncomms11598

503 22. Andersen, O.S.; Ingolfsson, H.I.; Lundbaek, J.A. Ion channels. *Wiley Encyclopedia of Chemical Biology*
504 **2008**, *1*–14. DOI: 10.1002/9780470048672.wecb259

505 23. Bezanilla, F. The voltage sensor in voltage-dependent ion channels. *Physiological Reviews* **2000**, *80*,
506 555–592. DOI: 10.1152/physrev.2000.80.2.555

507 24. Bezanilla, F. Voltage-gated ion channels. *IEEE Transactions on Nanobioscience* **2005**, *4*, 34–48. DOI:
508 10.1109/TNB.2004.842463

509 25. Bezanilla, F. How membrane proteins sense voltage. *Nature Reviews Molecular Cell Biology* **2008**, *9*,
510 323-331. DOI: 10.1038/nrm2376

511 26. Bezanilla, F. Ion channels: From conductance to structure. *Neuron* **2008**, *60*, 456-468. DOI:
512 10.1016/j.neuron.2008.10.035

513 27. Gonzalez, C.; Morera, F.J.; Rosenmann, E.; Alvarez, O.; Latorre, R. S3b amino acid residues do not
514 shuttle across the bilayer in voltage-dependent shaker K⁺ channels. *Proceedings of the National
515 Academy of Sciences* **2005**, *102*, 5020-5025. DOI: 10.1073/pnas.0501051102

516 28. Swartz, K.J. Sensing voltage across lipid membranes. *Nature* **2008**, *456*, 891-897. DOI:
517 10.1038/nature07620

518 29. Bryant, S.L.; Eixenberger, J.E.; Rossland, S.; Apsley, H.; Hoffmann, C.; Shrestha, N.; McHugh, M.;
519 Punnoose, A.; Fologea, D. ZnO nanoparticles modulate the ionic transport and voltage regulation of
520 lysenin nanochannels. *Journal of Nanobiotechnology* **2017**, *15*, 90. DOI: 10.1186/s12951-017-0327-9

521 30. Islas, L.D.; Sigworth, F.J. Electrostatics and the gating pore of Shaker potassium channels. *Journal of
522 General Physiology* **2001**, *117*, 69-89. DOI: 10.1085/jgp.117.1.69

523 31. Rappaport, S.M.; Teijido, O.; Hoogerheide, D.P.; Rostovtseva, T.K.; Berezhkovskii, A.M.; Bezrukov,
524 S.M. Conductance hysteresis in the voltage-dependent anion channel. *European Biophysics Journal*
525 **2015**, *44*, 465-472. DOI: 10.1007/s00249-015-1049-2

526 32. Xu, Y.P.; Shin, H.G.; Szep, S.; Lu, Z. Physical determinants of strong voltage sensitivity of K⁺ channel
527 block. *Nature Structural & Molecular Biology* **2009**, *16*, 1252-1258. DOI: 10.1038/nsmb.1717

528 33. Correa, A.M.; Bezanilla, F.; Latorre, R. Gating kinetics of batrachotoxin-modified Na⁺ channels in the
529 squid giant axon - voltage and temperature effects. *Biophysical Journal* **1992**, *61*, 1332-1352. DOI:
530 10.1016/s0006-3495(92)81941-0

531 34. Block, B.M.; Stacey, W.C.; Jones, S.W. Surface charge and lanthanum block of calcium current in
532 bullfrog sympathetic neurons. *Biophysical Journal* **1998**, *74*, 2278-2284. DOI:
533 10.1016/S0006-3495(98)77937-8

534 35. Bostrom, M.; Ninham, B.W. Energy of an ion crossing a low dielectric membrane: The role of
535 dispersion self-free energy. *Biophysical Chemistry* **2005**, *114*, 95-101. 10.1016/j.bpc.2004.11.003

536 36. Cherstvy, A.G. Electrostatic screening and energy barriers of ions in low-dielectric membranes.
537 *Journal of Physical Chemistry B* **2006**, *110*, 14503-14506. DOI: 10.1021/jp061745f

538 37. Glaeser, R.M.; Jap, B.K. The Born energy problem in bacteriorhodopsin. *Biophysical Journal* **1984**, *45*,
539 95-97. DOI: 10.1016/s0006-3495(84)84122-3

540 38. Parsegian, A. Energy of an ion crossing a low dielectric membrane: Solutions to four relevant
541 electrostatic problems. *Nature* **1969**, *221*, 844-846.

542 39. Jiang, Y.X.; Lee, A.; Chen, J.Y.; Ruta, V.; Cadene, M.; Chait, B.T.; MacKinnon, R. X-ray structure of a
543 voltage-dependent K⁺ channel. *Nature* **2003**, *423*, 33-41. DOI: 10.1038/nature01580

544 40. Jiang, Y.X.; Ruta, V.; Chen, J.Y.; Lee, A.; MacKinnon, R. The principle of gating charge movement in a
545 voltage-dependent K⁺ channel. *Nature* **2003**, *423*, 42-48. DOI: 10.1038/nature01581

546 41. Lee, A.G. Ion channels: A paddle in oil. *Nature* **2006**, *444*, 697-697. DOI: 10.1038/nature05408

547 42. Schmidt, D.; Jiang, Q.X.; MacKinnon, R. Phospholipids and the origin of cationic gating charges in
548 voltage sensors. *Nature* **2006**, *444*, 775-779. DOI: 10.1038/nature05416

549 43. Sigworth, F.J. Structural biology: Life's transistors. *Nature* **2003**, *423*, 21-22. DOI: 10.1038/423021a

550 44. Debye, V.P.; Huckel, E. Zur theorie der elektrolyte. *Physikalische Zeitschrift* **1923**, *24*, 185-206.

551 45. Solomon, T. The definition and unit of ionic strength. *Journal of Chemical Education* **2001**, *78*,
552 1691-1692. DOI: 10.1021/ed078p1691

553 46. Latorre, R.; Vargas, G.; Orta, G.; Brauchi, S. Voltage and temperature gating of thermoTRP channels.
554 In *TRP ion channel function in sensory transduction and cellular signaling cascades*, Liedtke, W.B., Heller,
555 S., Eds.; CRC Press/Taylor & Francis: Boca Raton (FL), USA, 2007; Chapter 21, 287-302.

556 47. Tao, X.; Lee, A.; Limapichat, W.; Dougherty, D.A.; MacKinnon, R. A gating charge transfer center in
557 voltage sensors. *Science* **2010**, *328*, 67-73. DOI: 10.1126/science.1185954

558

